MOLECULAR AND CELLULAR BIOLOGY, Dec. 1993, p. 7380–7392
0270-7306/93/127380-13$02.00/0

Vol. 13, No. 12

Activation of the Mouse *mdr3* Gene by Insertion of Retroviruses in Multidrug-Resistant P388 Tumor Cells

PIERRE LEPAGE,[1] ALAIN DEVAULT,[2] AND PHILIPPE GROS[1]*

Department of Biochemistry, McGill University, Montréal, Québec, Canada H3G 1Y6,[1] and Centre National de la Recherche Scientifique, Institut National de la Santé et de la Recherche Médicale, 34033 Montpellier Cedex, France[2]

Received 5 August 1993/Accepted 9 September 1993

In multidrug-resistant (MDR) derivatives of the mouse lymphoid tumor P388, the emergence of MDR is associated with overexpression and transcriptional activation of the *mdr3* gene, either in the absence of (P388/VCR-10) or concomitant with (P388/ADM-2) gene amplification. In both instances, Northern (RNA) blotting analyses have suggested the presence of altered *mdr3* transcripts in these cells, possibly originating from novel transcription initiation sites. The mechanisms underlying *mdr3* overexpression in these cells have been investigated. In P388/VCR-10 cells, Southern blotting analyses together with genomic DNA cloning and nucleotide sequencing have demonstrated the presence of an intact mouse mammary tumor virus (MMTV) within the boundaries of intron 1 of *mdr3*. cDNA cloning and nucleotide sequencing indicated that this integration event results in the synthesis and overexpression of a hybrid MMTV-*mdr3* mRNA which initiates within the U3 region of the 5′ long terminal repeat (LTR) of the provirus. Consequently, this mRNA lacks the normal exon 1 of *mdr3* but contains (i) MMTV LTR-derived sequences at its 5′ end, (ii) a novel *mdr3* exon, mapping within the boundaries of intron 1 downstream of the MMTV integration site and generated by alternative splicing, and (iii) an otherwise intact 3′ portion of *mdr3* starting at exon 2. A similar type of analysis of P388/ADM-2 cells revealed that *mdr3* overexpression in these cells is associated with the integration of an intracisternal A particle (IAP) within an L1Md repetitive element, immediately upstream of *mdr3*. The IAP insertion results in the overexpression of hybrid IAP-*mdr3* mRNA transcripts that initiate within the 3′ LTR of the IAP and which contain IAP LTR-derived sequences at the 5′ end spliced 14 nucleotides upstream of the normal exon 1 of *mdr3*. Taken together, these results indicate that independent retroviral insertions were the initial mutagenic event responsible for *mdr3* overexpression and survival during drug selection of these cell lines. Amplification of the rearranged and activated *mdr3* gene copy occurred during further selection for high-level drug resistance in P388/ADM-2 cells.

Expression of P-glycoprotein (P-gp), a phosphoglycoprotein of 170 kDa, causes multidrug resistance (MDR) in cultured cells in vitro and cancer cells in vivo (23, 28). P-gps are encoded by a small family of closely related genes, with two members *MDR1* and *MDR2* (also called *MDR3*) in humans and three members, *mdr1*, *mdr2*, and *mdr3*, in mice (7, 19, 30, 31, 76). The MDR phenotype is linked to an ATP-dependent decrease in cellular drug accumulation and increased drug efflux (18). The functional role of P-gps in drug resistance has been established in transfection experiments, in which sensitive cells acquire the MDR phenotype after expression of full-length cDNAs for either the mouse *mdr1*, mouse *mdr3*, or human *MDR1* gene (19, 29, 73). Human *MDR2* and mouse *mdr2* genes do not seem to play any role in MDR, as transfection and overexpression of these genes do not confer drug resistance (31, 67). Highly drug resistant MDR cell lines obtained by stepwise selection usually show very high levels of P-gp expression, associated with *mdr* gene overexpression and amplification (23). Cell lines with low-level drug resistance usually show increased P-gp expression either in the absence of gene amplification or from few *mdr* gene copies (3, 38, 45, 50, 62, 68). Enhanced transcriptional activity of the gene and increased stability or translation of the mRNA have been proposed to account for elevated P-gp expression in these cultured cells (38, 45, 46, 50, 68). In drug-resistant human tumor cells derived from tissues in which P-gp is not normally expressed, overexpression of *MDR1* mRNA and P-gp occurs in the absence of *MDR1* gene amplification (17, 35, 40, 65). It has been proposed either that MDR tumor cells expressing *MDR1* emerge after selection of preexisting cells (28) or that cytotoxic drugs may act directly or indirectly as positive regulators to increase *MDR1* mRNA expression (6). In cultured cells, *mdr* gene expression can be modulated by a number of factors and treatments, including exposure to differentiating agents (53), steroid hormones (2), arsenite (9), cytotoxic drugs (8, 41), P-gp antagonists (34), and heat shock treatment (9). Although several *cis*-acting sequences and *trans*-acting factors participating in constitutive and inducible *mdr* gene expression have been characterized in transient transfection assays for the human (10, 27, 50, 70, 74, 75) and rodent (15, 37, 39, 44, 46, 60, 61, 71, 72, 79) *mdr* gene promoters, the mechanisms responsible for increased *mdr* gene expression in cultured cells in vitro and tumor cells in vivo remain poorly understood.

Drug resistance in independently derived MDR mouse cell lines of lymphoid and fibroblastic origins has been found associated with independent overexpression of either *mdr1* or *mdr3* but not of *mdr2* (62). To study the mechanism underlying *mdr* gene overexpression in mouse MDR cells, the promoter region of the mouse *mdr3* gene was cloned and sequenced by our group (46) and other groups (37, 39). The transcription start site of *mdr3* has been mapped in MDR cells and in normal mouse tissues (37, 39). Several *cis*-regulatory elements, including consensus TATA and CAAT

* Corresponding author.

boxes as well as putative binding sites for transcription factors SP1, AP-1, and AP-2 (37, 39, 46), were identified. Only the AP-1 site has been shown to play a role in the regulation of *mdr3*, as this site functioned as a negative regulatory element in mouse hepatoma cells (39). In independent MDR isolates of the lymphoid tumor P388 (P388/SS), MDR is linked to the exclusive overexpression of *mdr3*, either from a single-copy gene (P388/VCR-10 and P388/ADM-1) or concomitant with gene amplification (P388/ADM-2) (62). In P388/VCR-10 cells, run-on transcription assays demonstrated that increased expression of *mdr3* was caused by a transcriptional activation of the gene (46). In addition, the *mdr3* transcripts overexpressed in these cells showed alterations at their 5′ end, including absence of exon 1 and presence of additional intron 1-derived sequences. Furthermore, in P388/ADM-2 cells, expression of *mdr3* mRNAs originated from two different start sites, one located 17 nucleotides (nt) upstream of the normal transcription start site and the other located further upstream (46). In these cells, the extent of gene expression far exceeds the level of gene amplification (62), suggesting that transcriptional activation of *mdr3* may together with gene amplification contribute to *mdr3* overexpression. In this study, we have further characterized the two independently derived MDR isolates, P388/VCR-10 and P388/ADM-2, and demonstrated that activation of *mdr3* in these cells was caused by insertion mutations, in which integration of active promoter sequences from two different retroviral elements induced expression of the gene.

MATERIALS AND METHODS

Cell culture. The mouse P388 lymphoid cell line and its drug-resistant derivatives, P388/ADM-2 and P388/VCR-10, were grown in suspension cultures in RPMI 1640 medium supplemented with 10% heat-inactivated fetal calf serum, L-glutamine (2 mM), streptomycin (50 μg/ml), and penicillin (50 U/ml). P388/ADM-2, a doxorubicin hydrochloride-resistant derivative obtained from G. Tarpley (Upjohn, Kalamazoo, Mich.), was grown in medium containing doxorubicin hydrochloride (Adriamycin; Adria Laboratories, Mississauga, Ontario, Canada) at 1.0 μg/ml. P388/VCR-10 and P388/VCR-20 are two subclones of the vincristine-resistant P388/VCR line (generous gift of D. Housman, Massachusetts Institute of Technology, Cambridge, Mass.) which were grown in medium containing vinblastine (Sigma Chemical Co., St. Louis, Mo.) at 10 and 20 ng/ml, respectively. We have previously established the specific drug resistance profiles of these cell lines, their degree of *mdr* gene amplification, and their levels of mRNA overexpression (62).

Southern hybridization. Genomic DNA was isolated from P388/SS, P388/VCR-10, and P388/ADM-2 cells according to standard procedures (66), using proteinase K (Gibco/BRL, Montreal, Quebec, Canada) treatment, sequential phenol and chloroform extractions, and ethanol precipitation. High-molecular-weight genomic DNA (or bacteriophage DNA) was digested to completion (37°C, 4 h), using a 10-fold excess of restriction endonucleases (10 U/μg of DNA) under conditions recommended by the supplier (Pharmacia/LKB, Montreal, Quebec, Canada). Digested DNA was electrophoresed in a 1% agarose gel containing 1× TAE (40 mM Tris acetate, 20 mM sodium acetate, 20 mM EDTA [pH 7.6]) and transferred by capillarity to a nylon hybridization membrane (Hybond-N; Amersham Corp., Arlington Heights, Ill.). Prehybridization was at 65°C for at least 4 h in 6× SSC (1× SSC is 0.15 M NaCl and 0.15 M sodium citrate)–5× Denhardt's solution (1× Denhardt's solution is 0.02% bovine serum albumin, 0.02% Ficoll, and 0.02% polyvinylpyrrolidone)–0.5% sodium dodecyl sulfate (SDS)–denatured salmon sperm DNA (200 μg/ml). Hybridization was in the same buffer containing 10^6 cpm of the ^{32}P-labelled probe per ml. Blots were washed to a final stringency of 0.1% SDS–0.2× SSC. The probes used were (i) intron −1 (I-1), produced by the polymerase chain reaction (PCR) using a pair of oligonucleotides flanking sequences upstream of the 5′ end of the *mdr3* gene (positions −192 to −40 with respect to the normal transcription start site) (46); and (ii) intron 1 to exon 2 (I1-E2) (positions +289 to +639), produced by PCR using two oligonucleotides, the first one mapping within the intron 1 of *mdr3* and of sequence 5′-CTGTGCTGTGGATCTCGC TG-3′ (positions +289 to +308) and the second one mapping at the 3′ end of the *mdr3* exon 2 on the complementary strand and of sequence 5′-CTCTTTTTGCCCATCTTTG AG-3′ (positions +639 to +619) (46). Probes were labelled to high specific activity (1×10^8 to 5×10^8 dpm/μg of DNA) with [α-^{32}P]dATP (3,000 Ci/mmol, Amersham), using the Klenow fragment of DNA polymerase I and random hexadeoxyribonucleotides (25).

Cloning the 5′ end of *mdr3* mRNA expressed in P388/VCR cells. Primer extension cDNA products were obtained by using P388/VCR-10 poly(A)$^+$ RNA and a synthetic oligonucleotide overlapping exon 2 of sequence 5′-GAAGTTCT TGTCTGCTCTTCCCTTAAGGTC-3′ (primer A in Fig. 2A; positions +619 to +590 on the complementary strand), as described previously (46). These cDNAs were cut out of a 5% polyacrylamide gel after visualization by autoradiography, eluted in 0.5 M ammonium acetate by constant agitation for 16 h at 37°C, and subjected to ethanol precipitation. To clone the primer extension product, a modification of the PCR-derived method, rapid amplification of cDNA ends (RACE) (26), was used. A poly(dA) tail was added to the 5′ end of the eluted products, using terminal deoxynucleotidyltransferase (30 U) under conditions recommended by the supplier (Gibco/BRL), and nucleic acids were recovered after phenol-chloroform extraction and ethanol precipitation. The poly(dA)-tailed single-stranded cDNA products were amplified by PCR using a synthetic oligonucleotide mapping within exon 2 and of sequence 5′-GCTCTTCCCT TAAGGTC-3′ (positions +607 to +590 on the complementary strand) and an adaptor oligonucleotide of sequence 5′-ATCGATCTCGAGTTTTTTTTTTTTTTT-3′) (primer B in Fig. 2A) as amplimers. The parameters for PCR were 1 min at 94°C, 1 min at 45°C, and 1 min at 72°C for 30 cycles. The PCR products were separated on a 1.5% low-melting-point agarose gel, and discrete fragments were eluted from the gel and used in a second round of amplification. For this second PCR, a third internal oligonucleotide mapping upstream of primer A within exon 2 and of sequence 5′-CTTCAAGTTCCATCACGAC-3′ (primer C in Fig. 2A; positions +587 to +569 on the complementary strand) was used in conjunction with the adaptor oligonucleotide (primer B). The parameters for the PCR were 1 min at 94°C, 1 min at 50°C, and 1 min at 72°C for 20 cycles. The PCR products were gel purified; their 5′ termini were repaired with T4 DNA polymerase and then cloned into the *Sma*I site of plasmid vector pUC18. The nucleotide sequence of the cloned PCR fragments was determined by the chain termination method using a modified T7 DNA polymerase (Sequenase; United States Biochemical Corp., Cleveland, Ohio).

Northern (RNA) blotting. Frozen cell pellets of P388/SS, P388/VCR-10, and P388/ADM-2 cells and of normal mouse

colon were dissolved in a solution containing 6 M guanidinium hydrochloride, and total RNA was purified by sequential ethanol precipitation (11). The polyadenylated mRNA fraction was obtained by chromatography on oligo(dT)-cellulose. One to 3 μg of poly(A)$^+$ RNA was electrophoresed in denaturing agarose gels containing 7% formaldehyde, and the RNA was transferred to a nylon hybridization membrane (GeneScreen Plus; DuPont NEN Research Products, Boston, Mass.) by capillary blotting in 10× SSC for 24 h and cross-linked to the membrane by UV irradiation. The blots were prehybridized at 60°C for 1 to 3 h in 7% SDS–5× SSPE (1× SSPE is 0.15 M NaCl, 0.001 M EDTA, and 0.01 M NaH_2PO_4 [pH 7.4])–10× Denhardt's solution–10% dextran sulfate–heat-denatured salmon sperm DNA (100 μg/ml). Hybridization was in the same buffer containing the ^{32}P-labelled oligonucleotide for 18 h at 60°C. The oligonucleotide probe used, of sequence 5′-CTTGCCGCGCCTGCAGCA GATATGGTTGAACTCCCGAG-3′, was derived from the complementary strand of the novel 5′-end sequence detected in the *mdr3* mRNA expressed in P388/VCR-10 cells (see Fig. 2B). The oligonucleotide probe was labelled with [γ-^{32}P]ATP (7,000 Ci/mmol; ICN, Montreal, Quebec, Canada), using T4 polynucleotide kinase under conditions recommended by the supplier (Pharmacia/LKB). The blots were washed once in 3× SSC–1× Denhardt's solution–5% SDS–0.025 M NaH_2PO_4 (pH 7.5) for 30 min at 60°C and once in 1% SDS–1× SSC for 30 min at the same temperature. The blots were exposed to Kodak XAR film for 16 h at −80°C with an intensifying screen.

Cloning of the MMTV provirus genomic DNA. A genomic DNA library was constructed by using DNA isolated from P388/VCR-10 cells. Genomic DNA was digested to completion with a 10-fold excess of *Sac*I (10 U/μg of DNA) under conditions recommended by the supplier (Pharmacia/LKB). The genomic DNA was size selected on a continuous sucrose gradient (10 to 40%, wt/vol), and fragments (10 to 20 kb in size) were inserted into the *Sac*I cloning site of the λDASH II bacteriophage vector (Stratagene, Edmonton, Alberta, Canada). The library was propagated in *Escherichia coli* host strain P2392, which allows direct selection of recombinant bacteriophages, and was screened with an *mdr3* genomic probe corresponding to I-1 (described above). This led to the identification of a bacteriophage containing a 12.5-kb *Sac*I insert fragment designated λMMDR3 and containing the entire mouse mammary tumor virus (MMTV) provirus flanked by *mdr3* sequences. A 1.2-kb *Hin*cII-*Sca*I fragment and a 1.5-kb *Pvu*II-*Sma*I fragment overlapping the 5′ and the 3′ MMTV/*mdr3* junctions, respectively, were subcloned into the *Sma*I site of M13mp18 and M13mp19 vectors. The nucleotide sequence of the 5′ and 3′ junctions was determined by the dideoxy-chain termination method, using modified T7 polymerase (Sequenase).

Cloning the 5′ end of *mdr3* mRNA expressed in P388/ADM-2 cells and determination of the integration site of an IAP. A cDNA library was constructed in bacteriophage λgt11 from poly(A)$^+$ RNA isolated from P388/ADM-2 cells, using a specific *mdr3* oligonucleotide primer (positions +1017 to +999 on the complementary strand, with respect to the translation initiator ATG) for reverse transcriptase-directed first-strand synthesis, as previously described (19). Clones overlapping the 5′ end of the *mdr3* mRNA overexpressed in these cells were identified by hybridization to a partial *mdr3* cDNA probe (19), and their nucleotide sequence was determined. Nucleotide sequencing of the 5′ end of these clones led to the identification of additional 5′ sequences that did not correspond to genomic DNA near the identified transcription start site of *mdr3*. These novel sequences were found to be identical to the long terminal repeat (LTR) of intracisternal A particle (IAP) retroviruses (24). To isolate genomic segments overlapping the IAP insertion site in *mdr3*, an IAP-specific oligonucleotide (5′-CCGCAGAAGATTCTGGTCTG-3′) (24) and an *mdr3*-specific oligonucleotide derived from sequences of the exon 1 (5′-GAGCCTTGGAAGATGGG-3′; positions +48 to +32 on the complementary strand) were used in a PCR. The template was P388/ADM-2 genomic DNA, and the reaction conditions were 94°C for 1 min, 50°C for 1 min, and 72°C for 2 min. A second round of PCR using the first PCR product as a template was carried out with the IAP LTR-specific oligonucleotide primer and a second *mdr3*-specific oligonucleotide derived from sequences upstream of exon 1 and of sequence (5′-GGTCAATTAGACAAACTC-3′) (positions −199 to −216 on the complementary strand). A unique PCR product was obtained, gel purified by electrophoresis on a 2% low-melting-point agarose gel, and inserted into a dT-tailed (52) *Eco*RV site of the pBluescript II KS(+) plasmid vector (Stratagene), and its nucleotide sequence was determined.

RESULTS

Southern blotting analysis of the 5′ end of *mdr3* in P388/VCR-10 and P388/ADM-2. We have shown by nuclear run-on transcription assay that the increased expression of *mdr3* mRNA and protein detected in P388/VCR-10 cells is caused by transcriptional activation of the gene (46). On the other hand, in P388/ADM-2 cells, the extent of *mdr3* mRNA overexpression far exceeds the level of gene amplification (seven to nine copies of the gene), suggesting that transcriptional activation of *mdr3* may also occur in these cells. Increased *mdr3* expression in these two cell lines is associated with the appearance of novel *mdr3* mRNAs with altered 5′ ends (46). Northern blot analyses using 5′ exon and intron *mdr3* probes have revealed the absence of the normal exon 1 and the presence of additional sequences derived from the intron 1 in the *mdr3* mRNAs overexpressed in P388/VCR-10 cells (46). RNase protection assays identified two novel *mdr3* transcription start sites used in P388/ADM-2 cells, one located 17 nt upstream of the normal start site used in normal mouse colon and a second located further upstream (46). To characterize the molecular basis of these altered *mdr3* mRNAs and to determine whether these alterations were related to transcriptional activation of the gene, we analyzed the integrity of genomic DNA sequences corresponding to the 5′ end of the *mdr3* mRNA. Genomic DNA from parental P388/SS and from P388/VCR-10 and P388/ADM-2 cells was digested to completion with *Eco*RI and analyzed by Southern blot analysis (Fig. 1) using a hybridization probe derived from sequences upstream of the exon 1 of *mdr3* (Fig. 1, solid bar in the diagram). This probe hybridized in all cell lines to a single-copy 2.8-kb genomic fragment defined by an *Eco*RI site located within a L1Md repetitive element upstream of the *mdr3* gene and a second *Eco*RI site located within intron 2 of the gene (Fig. 1). However, in P388/ADM-2 and P388/VCR-10 cells, additional hybridizing fragments of 5.9 kb (P388/ADM-2) and 6.4 kb (P388/VCR-10) were also detected by this probe, indicating that one of the two *mdr3* alleles is rearranged in these cells. While the rearranged allele of P388/VCR-10 cells (6.4 kb) produced a single-copy hybridization signal, the rearranged allele of P388/ADM-2 cells (5.9 kb) was present at several copies. This finding suggests that the rearranged *mdr3* copy is amplified in P388/ADM-2 cells

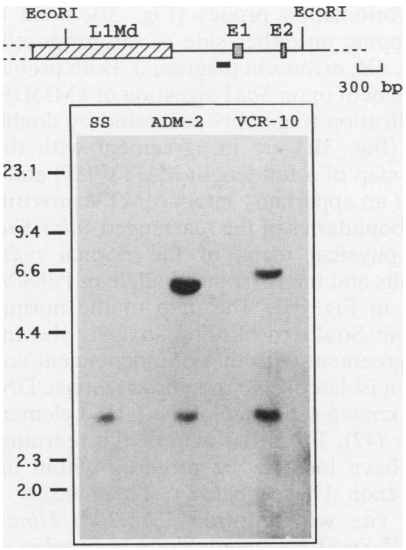

FIG. 1. Southern blotting analysis of the 5′ end region of *mdr3* in P388/SS, P388/ADM-2, and P388/VCR-10 cells. *Eco*RI-digested genomic DNA from P388/SS (SS), P388/ADM-2 (ADM-2), and P388/VCR-10 (VCR-10) cells was analyzed by using an *mdr3*-specific hybridization probe. A schematic representation of the 5′ region of the *mdr3* gene, encompassing part of an L1Md repetitive element, exon 1 (E1), and exon 2 (E2), is shown at the top. The hybridization probe used (I-1) is identified by a solid bar, and the two diagnostic *Eco*RI sites are shown. The probe detects on Southern blot a single hybridizing *Eco*RI fragment in all cell lines, whereas an additional rearranged hybridizing fragment is seen in P388/ADM-2 and in P388/VCR-10 DNAs. The *Hin*dIII fragments of bacteriophage λ are used as size markers. Sizes are indicated in kilobases.

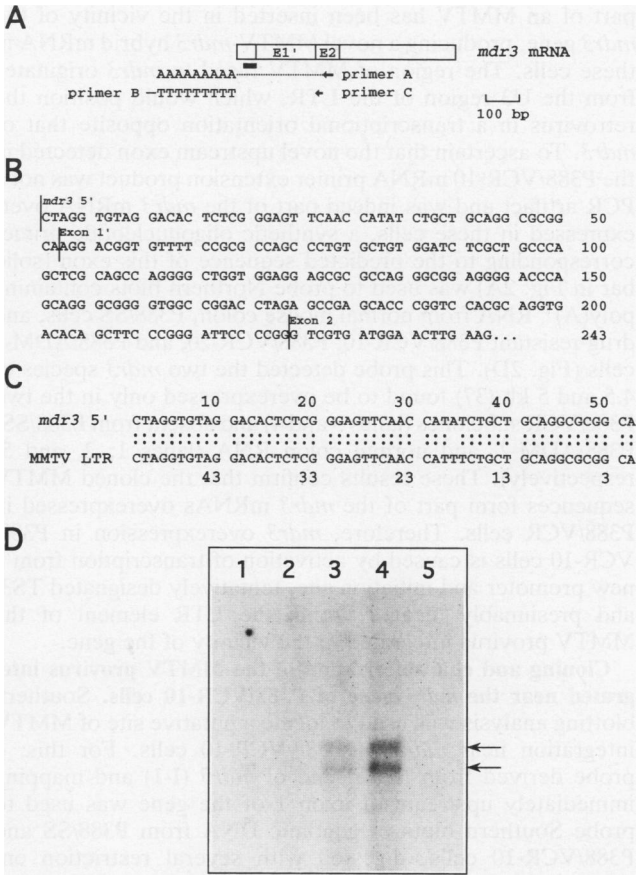

FIG. 2. Characterization of the 5′ end of *mdr3* mRNA transcripts overexpressed in P388/VCR-10 cells. (A) Strategy used to clone the 5′ end of the *mdr3* mRNA overexpressed in P388/VCR-10 cells (RACE). RNA from P388/VCR-10 cells was reverse transcribed into cDNA by using an *mdr3*-specific oligonucleotide derived from exon 2 (primer A), followed by addition of a poly(dA) tail at the 5′ end of the product by using terminal transferase. A complementary adaptor oligonucleotide with a poly(dT) tail at its 3′ end (primer B) was then used in conjunction with a second *mdr3*-specific oligonucleotide derived from exon 2 (primer C) to PCR amplify (RACE) an *mdr3*-specific product. (B) Nucleotide sequence of the 5′ end of *mdr3* mRNA from P388/VCR-10 amplified by RACE. Sequences derived from exon 2 and intron 1 (exon 1′) of *mdr3* are shown, together with the novel 52 nt of upstream sequences. Numbering is from the 5′ extremity of the cDNA. (C) Sequence alignment of the 52 nt from the 5′ end of *mdr3* mRNA transcripts in P388/VCR-10 cells with the MMTV LTR. Numbering for *mdr3* is as in panel B; numbering for MMTV is according to reference 55. (D) Northern blotting analysis of polyadenylated mRNA (2 μg) from P388/SS cells (lane 1), P388/ADM-2 cells (lane 2), two P388/VCR subclones (P388/VCR-10 [lane 3] and P388/VCR-20 [lane 4]), and normal mouse colon (lane 5). The blot was hybridized to an oligonucleotide probe derived from the 5′ end of the *mdr3* mRNA from P388/VCR-10 cells (solid bar in panel A). Arrows indicate the approximate 4.5- and 5.0-kb of the *mdr3* mRNAs overexpressed in the P388/VCR subclones.

and that the gene rearrangement preceded gene amplification in these cells. Taken together, these results indicate that *mdr3* overexpression in independently derived P388 MDR leukemic lines is linked to rearrangements near the 5′ end of *mdr3*.

Characterization of the 5′ end of the *mdr3* mRNAs overexpressed in P388/VCR-10 cells. We have previously shown by Northern blotting analysis that the 5′ extremity of *mdr3* mRNAs overexpressed in P388/VCR-10 cells lack exon 1 sequences but seem to contain additional sequences derived from intron 1. To further define these novel *mdr3* mRNAs and to delineate the transcription start site used in P388/VCR-10 cells, the 5′ end of *mdr3* mRNAs was isolated as a primer extension product, using a PCR-based approach (RACE) (26) followed by cloning and nucleotide sequencing (Fig. 2). Briefly, a specific oligonucleotide primer within exon 2 (primer A in Fig. 2A; positions +619 to +590 [46]) was used to direct reverse transcriptase-mediated elongation of poly(A)$^+$ RNA from P388/VCR-10 cells. Two products of approximately 240 and 250 nt were obtained (46) and subjected to PCR amplification, using an adaptor oligonucleotide (primer B) in conjunction with a second sequence-specific oligonucleotide within exon 2 (positions +587 to +569) (primer C). A predominant PCR product of approximately 250 bp in size was obtained, cloned, and sequenced (Fig. 2B). This fragment was found to contain expected exon 2 sequences at its 3′ end but appeared to contain two additional 5′ exons. The first one, designated exon 1′, maps entirely within the boundaries of intron 1 and consists of 172 nt spliced immediately upstream of exon 2. Consensus AG/GT splice sites are found immediately upstream and downstream of this novel exon. Upstream of exon 1′, an additional 52-nt segment corresponding to a novel exon was also identified. This novel exon showed no sequence homology to *mdr3* genomic sequences upstream of exon 1 but showed 98% identity to sequences derived from the LTR of MMTV (55) (Fig. 2C). This finding suggested that at least

part of an MMTV has been inserted in the vicinity of the *mdr3* gene, producing a novel MMTV-*mdr3* hybrid mRNA in these cells. The region of MMTV fused to *mdr3* originates from the U3 region of the LTR, which would position the retrovirus in a transcriptional orientation opposite that of *mdr3*. To ascertain that the novel upstream exon detected in the P388/VCR-10 mRNA primer extension product was not a PCR artifact and was indeed part of the *mdr3* mRNA overexpressed in these cells, a synthetic oligonucleotide primer corresponding to the predicted sequence of this exon (solid bar in Fig. 2A) was used to probe Northern blots containing poly(A)$^+$ RNA from normal mouse colon, P388/SS cells, and drug-resistant P388/VCR-10, P388/VCR-20, and P388/ADM-2 cells (Fig. 2D). This probe detected the two *mdr3* species of 4.5 and 5 kb (37) found to be overexpressed only in the two P388/VCR subclones (lanes 3 and 4) and absent from P388/SS, P388/ADM-2, and normal colon RNA (lanes 1, 2, and 5, respectively). These results confirm that the cloned MMTV sequences form part of the *mdr3* mRNAs overexpressed in P388/VCR cells. Therefore, *mdr3* overexpression in P388/VCR-10 cells is caused by activation of transcription from a new promoter and initiation site, tentatively designated TS3, and presumably located within the LTR element of the MMTV provirus integrated in the vicinity of the gene.

Cloning and characterization of the MMTV provirus integrated near the *mdr3* gene of P388/VCR-10 cells. Southern blotting analysis was used to locate a putative site of MMTV integration near *mdr3* in P388/VCR-10 cells. For this, a probe derived from the 5′ end of *mdr3* (I-1) and mapping immediately upstream of exon 1 of the gene was used to probe Southern blots of genomic DNA from P388/SS and P388/VCR-10 cells, digested with several restriction enzymes (Fig. 3A). Except for *Sph*I, which generated a single 8.8-kb hybridizing fragment in both cell lines, all restriction enzymes identified novel rearranged *mdr3* fragments in P388/VCR-10 cells: *Bam*HI, *Bgl*II, *Eco*RI, *Hin*dIII, *Kpn*I, *Pst*I, *Sac*I, and *Xba*I digestions produced *mdr3* fragments of 2.7, 4.2, 2.8, 3.8, 6.0, 8.6, 2.5, and 7.0 kb, respectively, in P388/SS cells, whereas additional rearranged *mdr3* fragments of 3.7, 4.4, 6.4, 6.6, 10.7, 7.9, 12.4, and 13.5 kb, respectively, were detected in P388/VCR-10 cells. Since a single *Sph*I site is located immediately downstream of the hybridization probe used (Fig. 3A and C), these results suggest that the *mdr3* genomic rearrangement identified in P388/VCR-10 cells has occurred within the interval defined by the *Sph*I site proximally and the *Eco*RI site distally (see Fig. 1). The presence of MMTV LTR sequences at the 5′ end of *mdr3* mRNA overexpressed in P388/VCR-10 cells, together with the known restriction map of MMTV and the Southern blotting analysis of the 5′ end of the rearranged *mdr3* gene copy (Fig. 3A), is compatible with the presence of an MMTV provirus integrated between the *Sph*I and *Eco*RI sites. According to this scheme, the size of the 12.4-kb *Sac*I fragment (arrow in Fig. 3A), the position of endogenous *Sac*I sites within normal genomic DNA (on either side of the *Sph*I and *Eco*RI sites; Fig. 3C), and the absence of *Sac*I sites in MMTV DNA (Fig. 3C) (55) together suggest that this 12.4-kb fragment may contain the entire integrated MMTV provirus. To verify this proposal and to further define the MMTV integration site, we cloned the rearranged 12.4-kb *Sac*I fragment from P388/VCR-10 cells in the corresponding site of λDASH II replacement vector, to generate clone λMMDR3. The restriction map of λMMDR3 was then constructed by Southern blotting using a series of restriction enzymes used in combination with *Sac*I and two *mdr3*-specific hybridization probes (Fig. 3B, solid bars in diagrams) mapping on either side of the proposed integration region (Fig. 3B, arrows in diagrams). Both probes detected a 12.4-kb fragment upon *Sac*I digestion of λMMDR3 (Fig. 3B). The hybridization fragments generated by double digests of λMMDR3 (Fig. 3B) are in agreement with the published restriction map of a full-length MMTV (55) and confirm the presence of an apparently intact MMTV provirus integrated within the boundaries of the rearranged *mdr3 Sac*I fragment. Compiled physical maps of the normal *mdr3* allele of P388/SS cells and the rearranged allele of P388/VCR-10 cells are shown in Fig. 3C. The map of the normal gene was derived from Southern blotting analysis shown in Fig. 3A and is in agreement with that of independent cosmid clones of the region isolated from the normal mouse DNA (45a) and that of the known sequence of the L1Md element located 5′ of the gene (47). From the map of the rearranged allele of *mdr3*, we have located the provirus within intron 1, upstream of exon 1′ (see below). To precisely identify the integration site within intron 1, 1.2-kb *Hin*cII-*Sca*I and 1.5-kb *Pvu*II-*Sma*I fragments likely to overlap the 5′ and 3′ junctions of the integration site, respectively, were gel purified, subcloned, and sequenced. Partial nucleotide sequence of these fragments identified the MMTV-*mdr3* junction points which are shown in Fig. 4. A 6-nt repeat originating from the host (AGGACG; underlined in Fig. 4A) is present on both sides of the provirus integration site. A 6-nt repeated sequence element from the host DNA is a hallmark of MMTV integration sites and has been previously described for MMTV integration at other unrelated loci (51). The integration site is located at position +270 in intron 1, immediately upstream of exon 1′ (Fig. 2B), and gives rise to a novel 5′ exon containing sequences derived from the U3 region of the MMTV 5′ LTR, with transcription possibly initiating at a site designated TS3 (Fig. 3C) and located well downstream of the transcription start site used in normal mouse tissues (TS1; Fig. 3C). This novel transcription start site (TS3) explains the absence of exon 1 sequences in the *mdr3* mRNA overexpressed in P388/VCR-10 cells (46). It is interesting to note that the MMTV 5′ LTR from which transcription would occur is in a transcriptional orientation opposite that of the *mdr3* gene. Taken together, our results indicate that *mdr3* transcriptional activation in P388/VCR-10 cells is caused by promoter activation due to MMTV insertion within intron 1 of the gene. The consequence of this integration event is the production of a hybrid *mdr3* mRNA transcript containing MMTV sequences at its 5′ end fused to *mdr3* intron 1 sequences (E1′) spliced to the downstream exon 2.

Characterization of the genomic rearrangement identified in the *mdr3* gene of P388/ADM-2 cells. To initiate the characterization of the *mdr3* genomic rearrangement identified in P388/ADM-2 cells, we sought to determined whether this rearrangement caused alterations in the 5′ end of *mdr3* mRNAs overexpressed in these cells. For this, we constructed a cDNA library using an *mdr3*-specific oligonucleotide mapping with the coding portion of the gene (positions +1017 to +999 on the complementary strand, with respect to the initiator ATG [19]) to prime first-strand cDNA synthesis of *mdr3* mRNA from P388/ADM-2 cells. *mdr3*-hybridizing clones with additional 5′ sequences extending beyond the normal transcription start site (TS1) were obtained, and the nucleotide sequence of the longest one was determined (Fig. 5). This clone was found to contain the complete sequence of exon 2 and exon 1 but to extend 103 nt upstream of the normal exon 1. The first 14 nt upstream of exon 1 in this

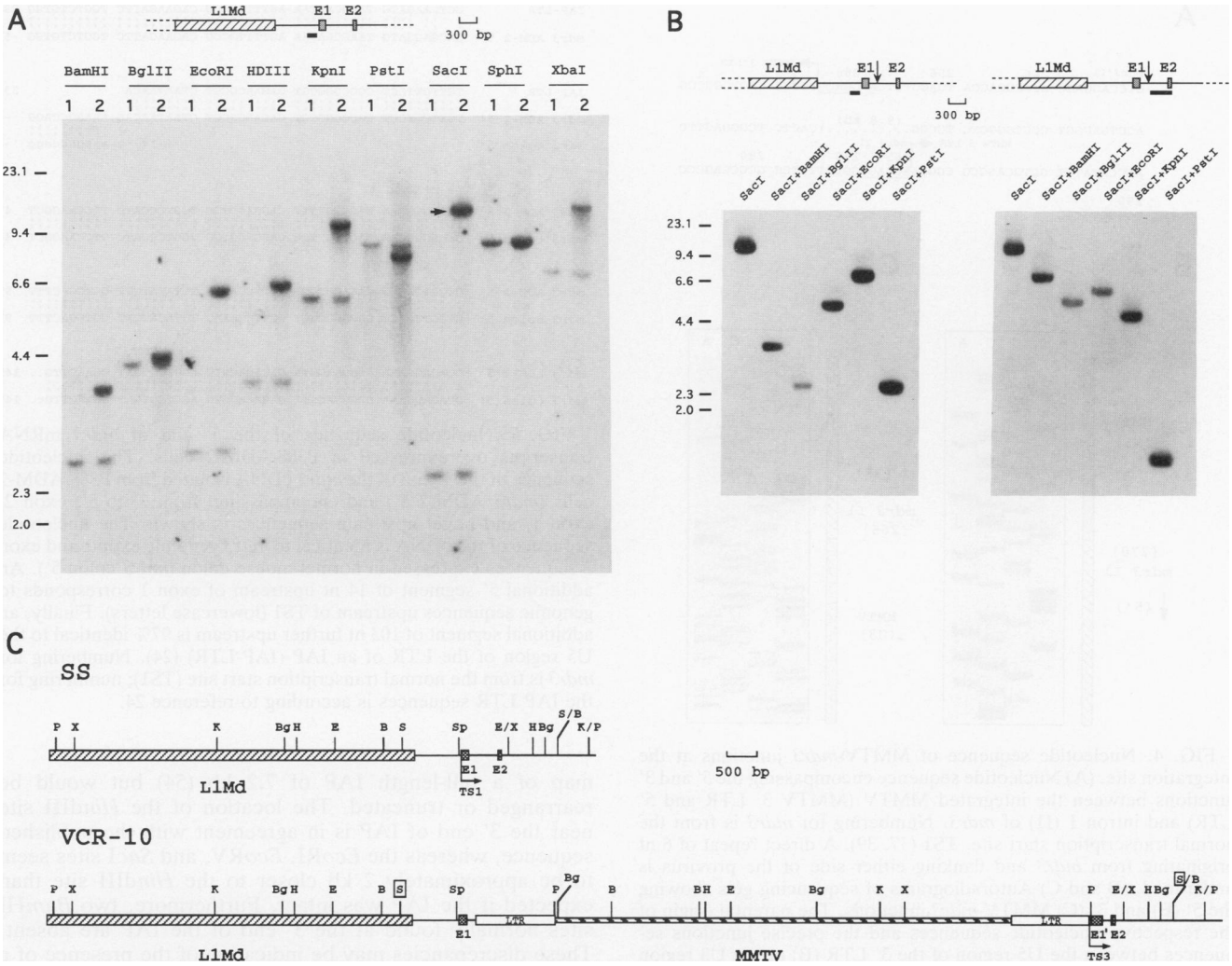

FIG. 3. Genomic organization of the 5′ end region of *mdr3* in P388/SS and P388/VCR-10 cells. (A) Southern blotting analysis of genomic DNA from P388/SS and P388/VCR-10 digested with restriction enzymes *Bam*HI, *Bgl*II, *Eco*RI, *Hin*dIII, *Kpn*I, *Pst*I, *Sac*I, *Sph*I, and *Xba*I. The blot was hybridized with probe I-1, which is identified as a solid bar in the diagram. This probe detects common hybridizing restriction fragments in both P388/SS (lanes 1) and P388/VCR-10 (lanes 2) cells, whereas additional hybridizing fragments are detected in P388/VCR-10 cells for all enzymes analyzed except *Sph*I. The arrow identifies the 12.4-kb *Sac*I P388/VCR-10 genomic fragment, containing a full-length MMTV, which was cloned in the unique *Sac*I site λDASH II vector to generate λMMDR3. (B) DNA from the λMMDR3 clone was digested with *Sac*I either alone or in combination with *Bam*HI, *Bgl*II, *Eco*RI, *Kpn*I, and *Pst*I, and analyzed by Southern blotting using two hybridization probes (solid bars in the diagrams) flanking the integration site on either side. The *Hin*dIII fragments of bacteriophage λ were used as size markers in panels A and B. Sizes are indicated in kilobases. (C) Restriction map of the 5′ region of *mdr3* in P388/SS and P388/VCR-10 cells deduced from Southern blotting analyses shown in panels A and B. The integration site of MMTV in P388/VCR-10 cells was located within intron 1 of the gene. The normal transcription start site of *mdr3* (TS1) and the approximate location of the novel transcription start site used in P388/VCR-10 (TS3) are shown. The novel 5′ exon (E1′) present in *mdr3* mRNA overexpressed in P388/VCR-10 cells and derived from normal intron 1 sequences is shown downstream of TS3. Restriction endonucleases used for mapping: B, *Bam*HI; Bg, *Bgl*II; E, *Eco*RI; H, *Hin*dIII; K, *Kpn*I; P, *Pst*I; S, *Sac*I; Sp, *Sph*I; X, *Xba*I. The two *Sac*I sites used to generate λMMDR3 are boxed.

clone showed 100% homology to *mdr3* genomic sequence immediately upstream of exon 1 (lowercase letters in Fig. 5), suggesting that the normal transcription start site (TS1) is not used for the synthesis of this novel mRNA in P388/ADM-2 cells. The additional 89 nt, however, shared no homology to *mdr3* genomic sequences but shared 97% (86 of 89 nucleotides) homology to a retrovirus-like LTR element. This sequence corresponds to the U5 region of the LTR (positions 250 to 338 [24]) of a family of murine defective retroviruses named IAP, which are present at approximately 1,000 copies in the normal mouse genome (48). This finding indicates that as in P388/VCR-10 cells, activation of *mdr3* expression in P388/ADM-2 cells may be linked to a retroviral insertional event in the 5′ end of the gene. To further investigate this possibility, genomic DNA from P388/SS and P388/ADM-2 cells was digested with different restriction enzymes and analyzed by Southern blotting using the *mdr3*-specific probe I-1 mapping immediately upstream of exon 1 of the gene (positions −192 to −40) (Fig. 6A, solid bar in the diagram). In P388/SS cells DNA (Fig. 6A, lanes 1), unique hybridizing fragments of 2.7, 2.8, 5.6, 3.8, and 2.5 kb were detected by probe I-1 upon digestion with *Bam*HI, *Eco*RI, *Eco*RV,

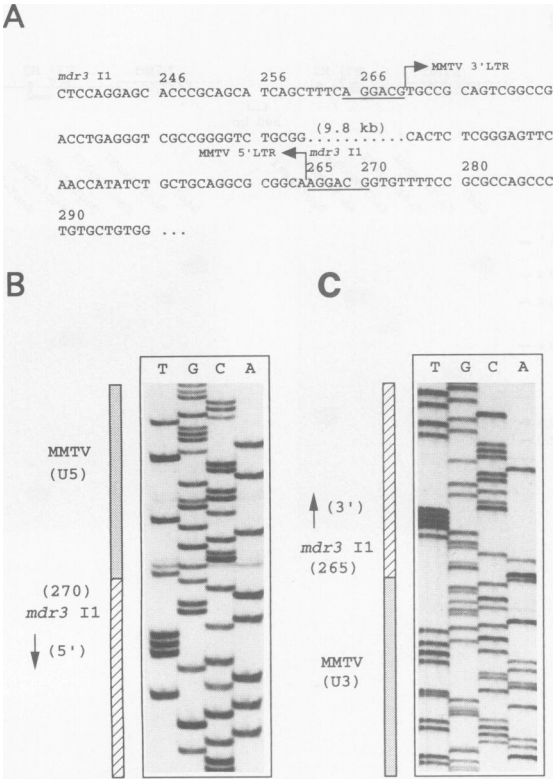

FIG. 4. Nucleotide sequence of MMTV-*mdr3* junctions at the integration site. (A) Nucleotide sequence encompassing the 5′ and 3′ junctions between the integrated MMTV (MMTV 3′ LTR and 5′ LTR) and intron 1 (I1) of *mdr3*. Numbering for *mdr3* is from the normal transcription start site, TS1 (37, 39). A direct repeat of 6 nt originating from *mdr3* and flanking either side of the provirus is underlined. (B and C) Autoradiograms of sequencing gels showing the 5′ (B) and 3′ (C) MMTV-*mdr3* junctions. The parental origin of the respective nucleotide sequences and the precise junctions sequences between the U5 region of the 3′ LTR (B) or the U3 region of the 5′ LTR (C) with *mdr3* intron 1 (I1) are shown at the left of each gel.

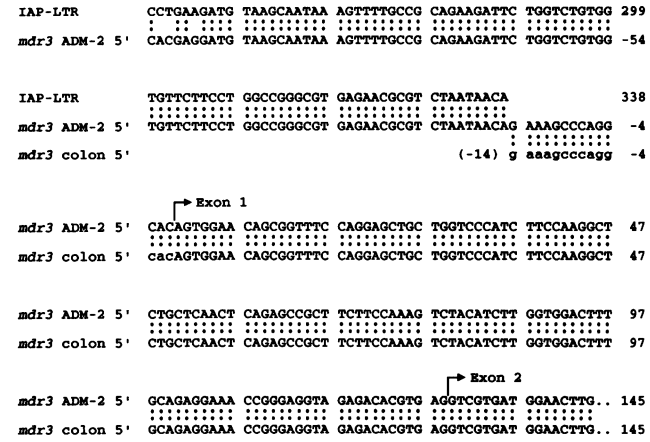

FIG. 5. Nucleotide sequence of the 5′ end of *mdr3* mRNA transcripts overexpressed in P388/ADM-2 cells. The nucleotide sequence of the 5′ end of the *mdr3* cDNA isolated from P388/ADM-2 cells (*mdr3* ADM-2 5′) and encompassing, from 3′ to 5′, exon 2, exon 1, and novel upstream sequences is shown. The nucleotide sequence of the cDNA is identical to *mdr3* genomic exon 1 and exon 2 sequences expressed in normal mouse colon (*mdr3* colon 5′). An additional 5′ segment of 14 nt upstream of exon 1 corresponds to genomic sequences upstream of TS1 (lowercase letters). Finally, an additional segment of 103 nt further upstream is 97% identical to the U5 region of the LTR of an IAP (IAP-LTR) (24). Numbering for *mdr3* is from the normal transcription start site (TS1); numbering for the IAP LTR sequences is according to reference 24.

*Hin*dIII, and *Sac*I, respectively, in agreement with the established restriction map of the normal *mdr3* gene. Digestion with the same enzymes produced an additional set of rearranged hybridizing fragments in P388/ADM-2 cells DNA (lanes 2) of 7.7, 5.7, 4.2, 2.9, and 5.5 kb. Interestingly, and as noted in Fig. 1, only rearranged fragments were found to be amplified in P388/ADM-2 genomic DNA. Digestion with *Nsi*I produced a single 2.6-kb amplified hybridizing fragment identical in size to that produced by the wild-type allele in P388/SS cells. Since a single *Nsi*I site is located 160 nt upstream of the 5′ end of the I-1 hybridization probe used, it appeared that the site of rearrangement in *mdr3* would be located within the interval defined by the *Nsi*I site distally and the *Sac*I site proximally (600 nt further upstream of the *Nsi*I site), since the *Sac*I genomic fragment detected by the I-1 probe is rearranged in P388/ADM-2 cells. A physical map of the rearranged fragment was established (Fig. 6B) on the basis of Southern blot analyses shown in Fig. 6A. The generated restriction map of this rearranged *mdr3* is compatible with the presence of an IAP integrated within the L1Md repeat located upstream of *mdr3* (Fig. 6B). However, this analysis also suggests that the integrated IAP is not intact, since its restriction map does not fit perfectly the predicted map of a full-length IAP of 7.2 kb (54) but would be rearranged or truncated. The location of the *Hin*dIII site near the 3′ end of IAP is in agreement with the published sequence, whereas the *Eco*RI, *Eco*RV, and *Sac*I sites seem to be approximately 2 kb closer to the *Hin*dIII site than expected if the IAP was intact. Furthermore, two *Bam*HI sites normally found at the 3′ end of the IAP are absent. These discrepancies may be indicative of the presence of a truncated IAP, missing a 2-kb DNA segment overlapping the two known *Bam*HI sites. The precise identification of the IAP by Southern blotting is complicated by the relative high degree of sequence heterogeneity amongst IAPs sequenced to date (49, 69). Nevertheless, taken together, these results strongly suggest that *mdr3* overexpression in P388/ADM-2 cells is linked to the presence of a retroviral IAP inserted in the promoter region of the gene.

Identification of the IAP insertion site within the 5′ end of *mdr3* in P388/ADM-2 cells. To precisely identify the integration site of IAP upstream of *mdr3* in P388/ADM-2 cells, we used a consensus oligonucleotide corresponding to the IAP LTR (Fig. 5, positions 277 to 296) together with an *mdr3*-specific primer mapping within exon 1 (positions +48 to +32 on the complementary strand) to PCR amplify the *mdr3* genomic fragment from P388/ADM-2 DNA containing the predicted *mdr3*-IAP junction point. A second round of PCR using the same IAP LTR-specific primer and a second *mdr3*-specific primer (positions −199 to −216 on the complementary strand), located upstream of exon 1, was used to generate a single specific fragment of approximately 700 nt (Fig. 7A, solid bar). This PCR fragment was gel purified, cloned, and sequenced. The structure of the rearranged gene is depicted in Fig. 7A, and a partial nucleotide sequence of the cloned PCR fragment, identifying the junction between IAP and *mdr3*, is shown in Fig. 7B and C. The integration site of the IAP is within the repetitive element L1Md and is

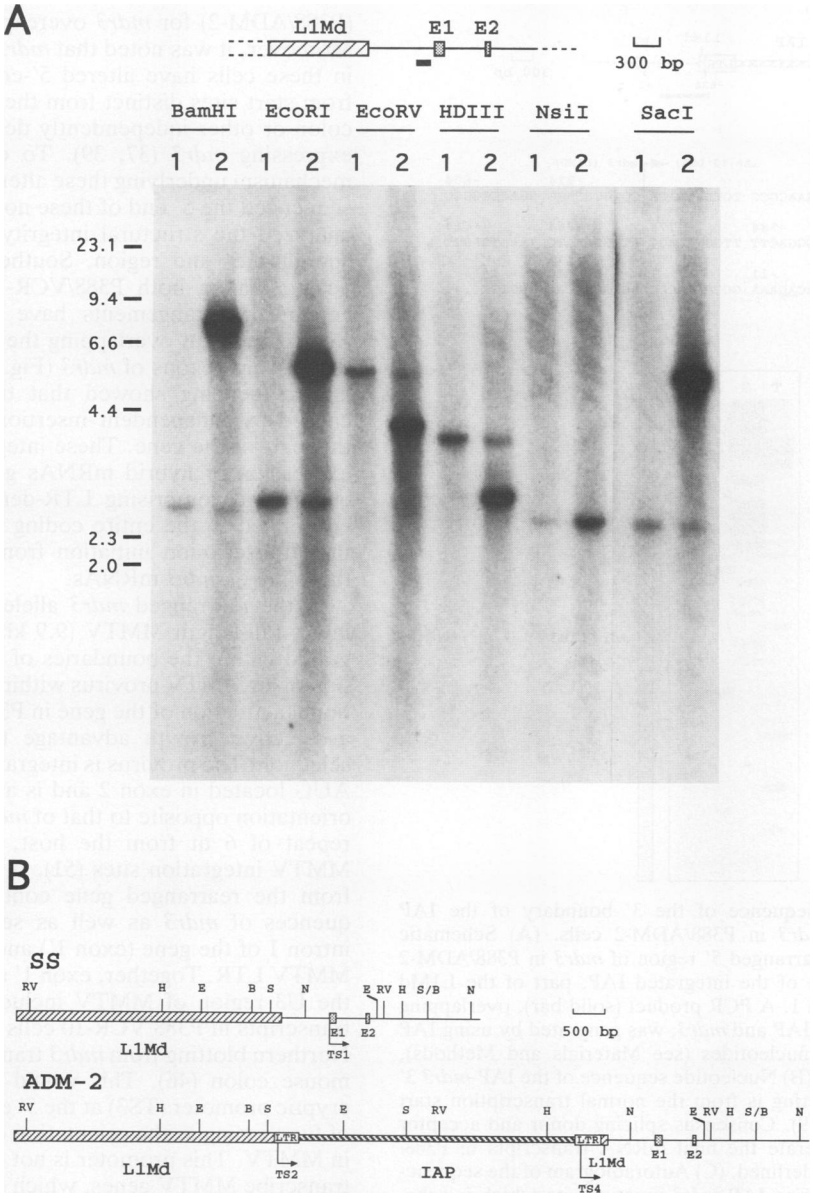

FIG. 6. Genomic organization of the 5′ end of *mdr3* in P388/ADM-2 cells. (A) Southern blotting analysis of genomic DNA from P388/SS (lanes 1) and P388/ADM-2 (lanes 2) cells, digested with restriction enzymes *Bam*HI, *Eco*RI, *Eco*RV, *Hin*dIII, *Nsi*I, and *Sac*I. The blot was hybridized with *mdr3* probe I-1, which is identified by a solid bar in the diagram. This probe identifies common hybridizing fragments in both P388/SS cells (lanes 1) and P388/ADM-2 cells, whereas additional hybridizing fragments are detected in P388/ADM-2 DNA (lanes 2) for all enzymes analyzed except *Nsi*I. The *Hin*dIII fragments of bacteriophage λ were used as size markers. Sizes are indicated in kilobases. (B) Restriction enzyme map of the 5′ region of *mdr3* in P388/SS (SS) and P388/ADM-2 (ADM-2) cells as deduced from Fig. 3 and Southern blotting analysis shown in panel A. The L1Md repetitive element and *mdr3* exon 1 (E1) and exon 2 (E2) are shown, together with the identified integrated IAP. The integration site of the IAP within the L1Md element was positioned by Southern blotting analysis in panel A and nucleotide sequencing of the 3′ IAP-*mdr3* junction (Fig. 7). The *mdr3* transcription start site used in normal mouse tissues (TS1) and in P388/ADM-2 cells (TS2 and TS4) are indicated. TS4 is located within the IAP 3′ LTR and direct synthesis of the 4.5-kb and 5.0-kb *mdr3* transcripts overexpressed in P388/ADM-2 cells (46). TS2 would be located within the IAP 5′ LTR and may direct synthesis of the large 9-kb *mdr3* mRNA transcript also overexpressed in P388/ADM-2 cells (46). Restriction endonucleases used for mapping: B, *Bam*HI; E, *Eco*RI; H, *Hin*dIII; N, *Nsi*I; RV, *Eco*RV; S, *Sac*I.

located 472 nt upstream of the *Nsi*I site, at position −824, in agreement with the predicted restriction map deduced in Fig. 6B. A comparison of the nucleotide sequence of the 5′ end of the *mdr3* transcript overexpressed in P388/ADM-2 cells (Fig. 5) with the genomic sequence of the IAP insertion site suggest that the *mdr3* mRNA initiates at a site identified here as TS4 (Fig. 6B) and located within the 3′ LTR of the IAP. This site is not yet precisely identified but may involve one of the 3′ LTR promoter elements (24). Mature *mdr3* mRNAs initiating at that site would be created by a splicing event with the 5′ splicing donor site located 2 nt downstream of the integration site of the IAP (Fig. 7B, position −823) and the 3′ splicing acceptor site located 14 nt upstream of the normal exon 1 (Fig. 7B, position −14). Taken together, these results

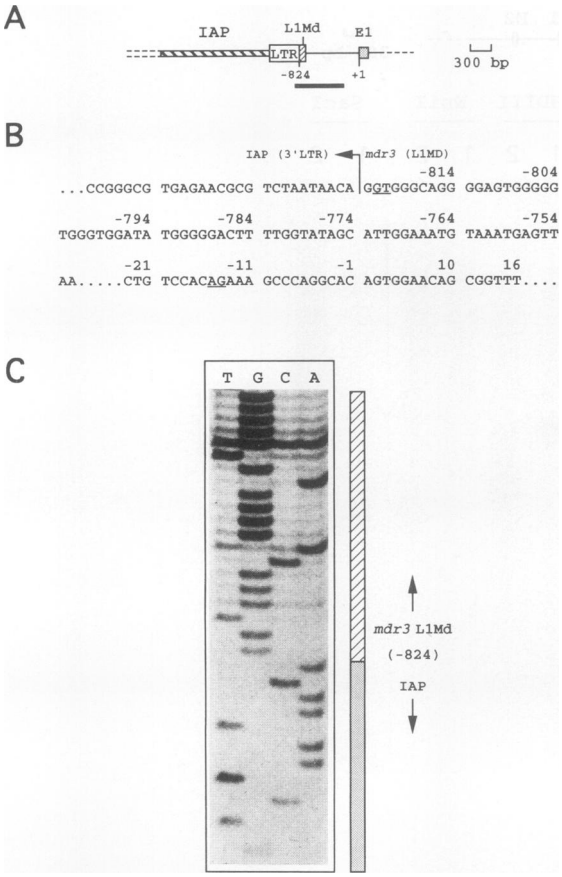

FIG. 7. Nucleotide sequence of the 3′ boundary of the IAP integration site near *mdr3* in P388/ADM-2 cells. (A) Schematic representation of the rearranged 5′ region of *mdr3* in P388/ADM-2 cells encompassing part of the integrated IAP, part of the L1Md element, and *mdr3* exon 1. A PCR product (solid bar), overlapping the 3′ junction between IAP and *mdr3*, was generated by using IAP and *mdr3*-specific oligonucleotides (see Materials and Methods), cloned, and sequenced. (B) Nucleotide sequence of the IAP-*mdr3* 3′ junction region. Numbering is from the normal transcription start site of *mdr3*, TS1 (37, 39). Consensus splicing donor and acceptor sequences used to generate the final mRNA transcripts in P388/ADM-2 (GT-AG) are underlined. (C) Autoradiogram of the sequencing gel showing the precise IAP-*mdr3* junction site which is schematized at the right as in Fig. 4.

indicate that overexpression of *mdr3* in P388/ADM-2 cells is caused by IAP insertion in the 5′ end of the gene and gene amplification. The insertion results in the overexpression of a hybrid IAP-*mdr3* mRNA initiating within and containing sequences derived from the 3′ LTR of the IAP.

DISCUSSION

The goal of this study was to elucidate the mechanism underlying *mdr3* overexpression in independently derived MDR isolates of the murine leukemic tumor line P388 (P388/SS). The three MDR isolates of this line, P388/VCR, P388/ADM-1, and P388/ADM-2, are characterized by overexpression of a single member (*mdr3*) of the *mdr* gene family from either a single copy (P388/VCR and P388/ADM-1) or amplified copies (P388/ADM-2) of the gene. We have shown previously that transcriptional activation of *mdr3* was directly responsible (P388/VCR-10) or highly likely to account (P388/ADM-2) for *mdr3* overexpression in these cells (46). Moreover, it was noted that *mdr3* transcripts overexpressed in these cells have altered 5′-end structures and originate from start sites distinct from the one used in normal mouse colon or other independently derived MDR cell lines overexpressing *mdr3* (37, 39). To characterize the molecular mechanism underlying these alterations, we have cloned and sequenced the 5′ end of these novel *mdr3* mRNAs and have analyzed the structural integrity of the gene in the corresponding 5′ end region. Southern blot analyses have revealed that in both P388/VCR-10 and P388/ADM-2 cells, genomic rearrangements have occurred within a 2.8-kb *Eco*RI fragment overlapping the transcription start site and the first two exons of *mdr3* (Fig. 1). Genomic DNA cloning and sequencing showed that these rearrangements were caused by independent insertion of retroviral elements in this part of the gene. These integrations result in high-level expression of hybrid mRNAs generated by novel splicing events and comprising LTR-derived sequences at their 5′ end linked to the entire coding region of *mdr3*, suggesting that transcription initiation from the viral LTR generates these novel *mdr3* mRNAs.

In the rearranged *mdr3* allele of P388/VCR-10 cells, an intact full-length MMTV (9.9 kb) provirus was found integrated within the boundaries of intron 1 (Fig. 3C). Integration of an MMTV provirus within *mdr3* resulted in transcriptional activation of the gene in P388/VCR-10 cells, providing a selective growth advantage to these cells during drug selection. The provirus is integrated upstream of the initiator AUG located in exon 2 and is arranged in a transcriptional orientation opposite to that of *mdr3*. It is flanked by a direct repeat of 6 nt from the host, which is characteristic of MMTV integration sites (51). A fusion transcript generated from the rearranged gene contains the entire coding sequences of *mdr3* as well as sequences derived from the intron 1 of the gene (exon 1′) and from the U3 region of the MMTV LTR. Together, exon 1′ and sequences derived from the U3 region of MMTV include 224 nt, generating *mdr3* transcripts in P388/VCR-10 cells of size indistinguishable by Northern blotting from *mdr3* transcripts expressed in normal mouse colon (46). This would suggest the presence of a cryptic promoter (TS3) at the 5′ end of the U3 region capable of functioning in the orientation opposite that normally seen in MMTV. This promoter is not the same as the one used to transcribe MMTV genes, which is located near the 3′ end of the U3 region, more than 1 kb distal (55). MMTV is a *cis*-acting oncovirus which causes mammary carcinomas in certain inbred strains of mice after insertion near and activation of cellular oncogenes (20, 58). At least five cellular proto-oncogenes have been shown to be activated after integration of an MMTV provirus. *wnt-1* (*int-1*) (58) and *wnt-3* (*int-4*) (64) are homologs of the *Drosophila wingless* gene, *fgf-3* (*int-2*) (20) and *hst/K-FGF* (59) are members of the fibroblast growth factor gene family, and *int-3* is a member of the *notch* gene family (63). The presence of a fusion MMTV LTR-*mdr3* transcript is indicative of an activation by promoter insertion, frequently seen in the case of avian leukemia virus integration (43) but rare in the case of MMTV (13). MMTV integration is generally upstream of the target gene in an antisense (3′ LTR to 5′ LTR) orientation or downstream of the target gene in a sense (5′ LTR to 3′ LTR) orientation (13). However, it is unusual that an MMTV integrated in the antisense orientation upstream of a gene leads to the production of fusion transcripts. MMTV provirus are frequently found upstream of *wnt-1* or *fgf-3* genes in the antisense orientation, where they have been shown to

up-regulate the normal promoter of these genes as a result of the presence of an enhancer element within the LTR region (57). Nevertheless, two cases have been documented (21, 56) in which the integration of an MMTV in the antisense orientation disrupted the normal promoter of the activated gene, suggesting the presence of a cryptic promoter in the U3 region capable of functioning in the opposite orientation. Our findings on MMTV integration in *mdr3* in P388/VCR-10 cells are in agreement with this proposal. The activation of a gene by an antisense LTR has also been noted in the case of the retrovirus-like element IAP, found to activate c-*mos* (36) and also the interleukin-3 gene (33). Even though no gross rearrangement of the integrated MMTV provirus were detected in our study (Fig. 3C), the possibility that the LTR region of the provirus has undergone a small rearrangement leading to the appearance of a novel promoter in that region cannot yet be excluded. Deletions of about 500 nt similar to the ones noted in the LTR of MMTV causing T-cell lymphomas (77) were not seen here, as shown by the size of a 1.5-kb *Pvu*II-*Sma*I fragment containing the entire 1.3-kb 3′ LTR.

We have determined that in P388/ADM-2 cells, an IAP was integrated 824 nt upstream of the normal *mdr3* transcription start site, within a L1Md mouse repetitive element (Fig. 6B). IAP is a defective retrovirus-like element, or retrotransposon, which is present at approximately 1,000 copies per mouse haploid genome (48). Integration of this element in the vicinity of certain genes was found to up- or down-regulate their normal level or pattern of expression. IAP integrated in the κ light-chain immunoglobulin gene disrupted the expression of that gene (32), whereas IAPs integrated upstream or downstream of c-*mos* (16), *hox-2.4* (5), or the interleukin-3 (1, 78) or interleukin-6 (4) gene caused the overexpression of these genes either by transcriptional activation (4, 5, 16, 78) or by stabilization of the gene transcript (1). In vitro studies have clearly established that the promoters of some IAPs can be bidirectional, working in both the sense and antisense orientations, whereas promoters of other IAPs work only in the sense orientation (12). The IAP integrated upstream *mdr3* in P388/ADM-2 cells is in the sense orientation and, as for the MMTV provirus in P388/VCR-10 cells, provided a growth advantage to these cells during selection in drug-containing medium. Interestingly, Southern blot analyses (Fig. 6A) indicated that only the rearranged IAP-containing allele of *mdr3* was amplified in these cells. This finding suggests that IAP integration leading to *mdr3* transcriptional activation was the initial mutagenic event during drug selection, which was followed by gene amplification upon subsequent stepwise selection for high-level drug resistance in these cells. The integration of IAP in the sense orientation upstream of *mdr3* leads to the production of a fusion transcript with sequences derived from the U5 region of the IAP LTR, fused to genomic sequences which include 13 nt upstream of exon 1 and the entire exon 1 of *mdr3* (Fig. 5). This transcript may initiate at the junction of the U3 and R regions in the 3′ LTR (TS4), which is the known IAP transcription start site produced from the promoter located in the U3 region (24). The novel intron upstream of exon 1 is flanked by a 5′ splice donor site immediately downstream of the integration site (from position −823) and a 3′ splice acceptor site upstream of the extended exon 1 (up to position −14) (Fig. 7B). The novel splicing event described here is in agreement with our previous identification of an altered *mdr3* transcription start site in P388/ADM-2 cells detected by RNase protection using cRNA probes derived from the region (46) (in fact, identifying the 5′ boundary of extended exon 1). The possibility that IAP-*mdr3* fusion transcripts detected in P388/ADM-2 cells could be generated by splicing of mRNAs initiating within the 5′ LTR of the IAP cannot be formally excluded. Finally, transcription initiation within the 5′ LTR may also produce, by readthrough of the IAP element, a large *mdr3* transcript of over 9 kb (initiating from TS2) which we have also detected in these cells (46). According to the physical map (Fig. 6B), the IAP integrated near *mdr3* contains a deletion of approximately 2 kb, compared with the full-length type I IAP, which is 7.2 kb (54). This deleted portion encompasses two *Bam*HI sites near the 3′ end of the element and may be the same variant that was detected in a cDNA isolated from a T-cell hybridoma (54). This variant was designated IΔ2 and is the only known variant with a deletion encompassing the two *Bam*HI sites near the 3′ end of IAP (42).

Taken together, these results indicate that overexpression of *mdr3* in the two drug-resistant P388 derivatives analyzed here is caused by the insertion of active promoter/enhancer elements upstream of the gene. A third MDR isolate of P388, P388/ADM-1, was previously shown to also overexpress *mdr3* from a single copy of the gene (62). Southern blotting analysis using an *mdr3*-specific probe derived from the 5′ region of the gene also revealed an altered *mdr3* allele rearranged in the same *Eco*RI fragment disrupted in P388/VCR-10 and P388/ADM-2 cells (not shown). In addition to the normal 2.8-kb *Eco*RI fragment, an additional 2.4-kb *Eco*RI fragment was detected in P388/ADM-1 cells, indicating that the gene rearrangement observed in these cells is independent from those of P388/VCR-10 and P388/ADM-2 cells (Fig. 1). Although the rearrangement seen in P388/ADM-1 cells awaits further characterization, the observation that a third P388-derived MDR cell line shows a genomic rearrangement near *mdr3* suggests that promoter disruption and recruitment of strong *cis*-acting promoter/enhancer elements is required to activate the otherwise silent *mdr3* gene in P388 cells. Indeed, expression of *mdr3* mRNAs could not be detected in parental P388/SS cells, even with a very sensitive PCR-based method (not shown), suggesting a lack of an essential *trans*-acting factor required for *mdr3* transcription or indicative of active repression of *mdr3* in P388 cells. Retroviral sequences inserted in *cis* could relieve negative regulation of the gene by disrupting the normal architecture of the promoter region required for active repression, or this new promoter/enhancer complex could be active even in absence of a key positive regulator of *mdr3*. It is interesting to note that only *mdr3* and not the other biologically active *mdr1* gene is overexpressed in all MDR derivatives of P388 cells analyzed to date, even when both genes are amplified, as is the case for P388/ADM-2 cells. It is tempting to speculate that the L1Md element found upstream of the *mdr3* gene (but not in *mdr1*) may contribute to local genomic instability and favor the integration of retroviral elements near the 5′ end of the gene. Indeed, MMTV integration sites are often located near an L1Md element throughout the mouse genome (22). This situation would lead to preferential retrovirus-mediated activation of the *mdr3* rather than *mdr1* gene in these cells. Interestingly, in a taxol-resistant MDR isolate (J7.T1-50) of the macrophage line J774.2, a genomic rearrangement upstream of *mdr3* (*mdr1a*), implicating part of the *mdr1* gene and the *mdr3* L1Md element, has been described (14).

ACKNOWLEDGMENTS

We thank N. Sonenberg, G. Shore, and A. Underhill (McGill University) for helpful comments and discussions throughout this

work. We are indebted to G. Tarpley (The Upjohn Co., Kalamazoo, Mich.) and D. Housman for gifts of cell lines.

This work was supported by grants to P.G. from the Medical Research Council of Canada and the Howard Hughes Medical Institute. P.G. is supported by a career award from the Fonds de Recherche en Santé du Québec (FRSQ); P.L. is supported by a studentship from FRSQ.

REFERENCES

1. **Algate, P. A., and J. A. McCubrey.** 1993. Autocrine transformation of hemopoietic cells resulting from cytokine message stabilization after intracisternal A particle transposition. Oncogene **8**:1221–1232.
2. **Arceci, R. J., F. Baas, R. Raponi, S. B. Horwitz, D. Housman, and J. M. Croop.** 1990. Multidrug resistance gene expression is controlled by steroid hormones in the secretory epithelium of the uterus. Mol. Reprod. Dev. **25**:101–109.
3. **Bénard, J., J. Da Silva, J.-R. Teyssier, and G. Riou.** 1989. Over-expression of *MDR1* gene with no DNA amplification in a multiple-drug-resistant human ovarian carcinoma cell line. Int. J. Cancer **43**:471–477.
4. **Blankenstein, T., Z. Qin, W. Li, and T. Diamantstein.** 1990. DNA rearrangement and constitutive expression of the interleukin 6 gene in a mouse plasmacytoma. J. Exp. Med. **171**:965–970.
5. **Blatt, C., D. Aberdam, R. Schwartz, and L. Sachs.** 1988. DNA rearrangement of a homeobox gene in myeloid leukemia cells. EMBO J. **7**:4283–4290.
6. **Chaudhary, P. M., and I. B. Roninson.** 1993. Induction of multidrug resistance in human cells by transient exposure to different chemotherapeutic drugs. J. Natl. Cancer Inst. **85**:632–639.
7. **Chen, C.-J., J. E. Chin, K. Ueda, D. P. Clark, I. Pastan, M. M. Gottesman, and I. B. Roninson.** 1986. Internal duplication and homology with bacterial transport proteins in the *mdr1* (P-glycoprotein) gene from human multidrug-resistant cells. Cell **47**:381–389.
8. **Chin, K.-V., S. S. Chauhan, I. Pastan, and M. M. Gottesman.** 1990. Regulation of the *mdr* RNA levels in response to cytotoxic drugs in rodent cells. Cell Growth Differ. **1**:361–365.
9. **Chin, K.-V., S. Tanaka, G. Darlington, I. Pastan, and M. M. Gottesman.** 1990. Heat shock and arsenite increase expression of the multidrug resistance (*MDR1*) gene in human renal carcinoma cells. J. Biol. Chem. **265**:221–226.
10. **Chin, K.-V., K. Ueda, I. Pastan, and M. M. Gottesman.** 1992. Modulation of activity of the promoter of the human *MDR1* gene by *ras* and *p53*. Science **255**:459–462.
11. **Chirgwin, J. M., A. A. Przybyla, R. J. MacDonald, and W. J. Rutter.** 1979. Isolation of biologically active ribonucleic acid from sources enriched in ribonuclease. Biochemistry **18**:5294–5306.
12. **Christy, R. J., and R. C. C. Huang.** 1988. Functional analysis of the long terminal repeats of intracisternal A-particle genes: sequences within the U3 region determine both the efficiency and direction of promoter activity. Mol. Cell. Biol. **8**:1093–1102.
13. **Clausse, N., D. Baines, R. Moore, S. Brookes, C. Dickson, and G. Peters.** 1993. Activation of both *wnt-1* and *fgf-3* by insertion of mouse mammary tumor virus downstream in the reverse orientation: a reappraisal of the enhancer insertion model. Virology **194**:157–165.
14. **Cohen, D., S. M. Higman, S. I.-H. Hsu, and S. B. Horwitz.** 1992. The involvement of a LINE-1 element in a DNA rearrangement upstream of the *mdr*1a gene in a taxol multidrug-resistant murine cell line. J. Biol. Chem. **267**:20248–20254.
15. **Cohen, D., R. L. Piekarz, S. I.-H. Hsu, R. A. DePinho, N. Carrasco, and S. B. Horwitz.** 1991. Structural and functional analysis of the mouse *mdr*1b gene promoter. J. Biol. Chem. **266**:2239–2244.
16. **Cohen, J. B., T. Unger, G. Rechavi, E. Canaani, and D. Givol.** 1983. Rearrangement of the oncogene c-*mos* in mouse myeloma NSI and hybridomas. Nature (London) **306**:797–799.
17. **Corrias, M. V., P. Cornaglia-Ferraris, D. Di Martino, A. M. Stenger, E. Lanino, L. Boni, and G. P. Tonini.** 1990. Expression of multiple drug resistance gene, *MDR1*, and N-*myc* oncogene in an Italian population of human neuroblastoma patients. Anticancer Res. **10**:897–902.
18. **Danø, K.** 1973. Active outward transport of daunomycin in resistant Ehrlich ascites tumor cells. Biochim. Biophys. Acta **323**:466–483.
19. **Devault, A., and P. Gros.** 1990. Two members of the mouse *mdr* gene family confer multidrug resistance with overlapping but distinct drug specificities. Mol. Cell. Biol. **10**:1652–1663.
20. **Dickson, C., R. Smith, S. Brookes, and G. Peters.** 1984. Tumorigenesis by mouse mammary tumor virus: proviral activation of a cellular gene in the common integration region *int-2*. Cell **37**:529–536.
21. **Dickson, C., R. Smith, S. Brookes, and G. Peters.** 1990. Proviral insertions within the *int-2* gene can generate multiple anomalous transcripts but leave the protein-coding domain intact. J. Virol. **64**:784–793.
22. **Dudley, J. P.** 1988. Mouse mammary tumor proviruses from a T-cell lymphoma are associated with the retroposon L1Md. J. Virol. **62**:472–478.
23. **Endicott, J. A., and V. Ling.** 1989. The biochemistry of P-glycoprotein-mediated multidrug resistance. Annu. Rev. Biochem. **58**:137–171.
24. **Falzon, M., and E. L. Kuff.** 1988. Multiple protein-binding sites in an intracisternal A particle long terminal repeat. J. Virol. **62**:4070–4077.
25. **Feinberg, A. P., and B. Vogelstein.** 1984. A technique for radiolabelling DNA restriction endonuclease fragments to high specific activity. Anal. Biochem. **137**:266–267.
26. **Frohman, M. A., M. K. Dush, and G. R. Martin.** 1988. Rapid production of full-length cDNAs from rare transcripts: amplification using a single gene-specific oligonucleotide primer. Proc. Natl. Acad. Sci. USA **85**:8998–9002.
27. **Goldsmith, M. E., M. J. Madden, C. S. Morrow, and K. H. Cowan.** 1993. A Y-box consensus sequence is required for basal expression of the human multidrug resistance (*mdr*1) gene. J. Biol. Chem. **268**:5856–5860.
28. **Gottesman, M. M., and I. Pastan.** 1993. Biochemistry of multidrug resistance mediated by the multidrug transporter. Annu. Rev. Biochem. **62**:385–427.
29. **Gros, P., Y. Ben-Neriah, J. M. Croop, and D. E. Housman.** 1986. Isolation and expression of complementary DNA that confers multidrug resistance. Nature (London) **323**:728–731.
30. **Gros, P., J. Croop, and D. Housman.** 1986. Mammalian multidrug resistance gene: complete cDNA sequence indicates strong homology to bacterial transport proteins. Cell **47**:371–380.
31. **Gros, P., M. Raymond, J. Bell, and D. Housman.** 1988. Cloning and characterization of a second member of the mouse *mdr* gene family. Mol. Cell. Biol. **8**:2770–2778.
32. **Hawley, R. G., M. J. Shulman, and N. Hozumi.** 1984. Transposition of two different intracisternal A particle elements into an immunoglobulin kappa-chain gene. Mol. Cell. Biol. **4**:2565–2572.
33. **Heberlein, C., M. Kawai, M.-J. Franz, G. Beck-Engeser, C. P. Daniel, W. Ostertag, and C. Stocking.** 1990. Retrotransposons as mutagens in the induction of growth autonomy in hematopoietic cells. Oncogene **5**:1799–1807.
34. **Herzog, C. E., M. Tsokos, S. E. Bates, and A. T. Fojo.** 1993. Increased *mdr*-1/P-glycoprotein expression after treatment of human colon carcinoma cells with P-glycoprotein antagonists. J. Biol. Chem. **268**:2946–2952.
35. **Holmes, J., A. Jacobs, G. Carter, A. Janowska-Wieczorek, and R. A. Padua.** 1989. Multidrug resistance in haemopoietic cell lines, myelodysplastic syndromes and acute myeloblastic leukaemia. Br. J. Cancer **72**:40–44.
36. **Horowitz, M., S. Luria, G. Rechavi, and D. Givol.** 1984. Mechanism of activation of the mouse c-*mos* oncogene by the LTR of an intracisternal A-particle gene. EMBO J. **3**:2937–2941.
37. **Hsu, S. I.-H., D. Cohen, L. S. Kirchner, M. Hartstein, and S. B. Horwitz.** 1990. Structural analysis of the mouse *mdr1a* (P-glycoprotein) promoter reveals the basis for differential transcript heterogeneity in multidrug-resistant J774.2 cells. Mol. Cell. Biol. **10**:3596–3606.
38. **Hsu, S. I.-H., L. Lothstein, and S. B. Horwitz.** 1989. Differential

overexpression of three *mdr* gene family members in multidrug-resistant J774.2 mouse cells. J. Biol. Chem. **264**:12053–12062.
39. **Ikeguchi, M., L. D. Teeter, T. Eckersberg, R. Ganapathi, and M. T. Kuo.** 1991. Structural and functional analyses of the promoter of the murine multidrug resistance gene *mdr3/mdr1a* reveal a negative element containing the AP-1 binding site. DNA Cell Biol. **10**:639–649.
40. **Ito, Y., M. Tanimoto, T. Kumazawa, M. Okumura, Y. Morishima, R. Ohno, and H. Saito.** 1989. Increased P-glycoprotein expression and multidrug-resistant gene (*mdr1*) amplification are infrequently found is fresh acute leukemia cells. Cancer **63**:1534–1538.
41. **Kohno, K., S. Sato, H. Takano, K. Matsuo, and M. Kuwano.** 1989. The direct activation of human multidrug resistance gene (*MDR1*) by anticancer agents. Biochem. Biophys. Res. Commun. **165**:1415–1421.
42. **Kuff, E. L., and K. K. Lueders.** 1988. The intracisternal A-particle gene family: structure and functional aspects. Adv. Cancer Res. **51**:183–276.
43. **Kung, H.-J., C. Boerkoel, and T. H. Carter.** 1991. Retroviral mutagenesis of cellular oncogenes: a review with insights into the mechanisms of insertional mutation. Curr. Top. Microbiol. Immunol. **171**:1–25.
44. **Kuo, M. T., J.-Y. Zhao, L. D. Teeter, M. Ikeguchi, and F. V. Chisari.** 1992. Activation of multidrug resistance (P-glycoprotein) *mdr3/mdr1a* gene during the development of hepatocellular carcinoma in hepatitis B virus transgenic mice. Cell Growth Differ. **3**:531–540.
45. **Lemontt, J. F., M. Azzaria, and P. Gros.** 1988. Increased *mdr* gene expression and decreased drug accumulation in multidrug-resistant human melanoma cells. Cancer Res. **48**:6348–6353.
45a. **Lepage, P., and P. Gros.** Unpublished data.
46. **Lepage, P., M. Raymond, A. Nepveu, and P. Gros.** 1993. Transcriptional activation of the mouse *mdr3* gene coincides with the appearance of novel transcription initiation sites in multidrug-resistant P388 tumor cells. Cancer Res. **53**:1657–1664.
47. **Loeb, D. D., R. W. Padgett, S. C. Hardies, W. R. Shehee, M. B. Comer, M. H. Edgell, and C. A. Hutchison III.** 1986. The sequence of a large L1Md element reveals a tandemly repeated 5′ end and several features found in retrotransposons. Mol. Cell. Biol. **6**:168–182.
48. **Lueders, K. K., and E. L. Kuff.** 1977. Sequences associated with intracisternal A-particles are reiterated in the mouse genome. Cell **12**:963–972.
49. **Lueders, K. K., and J. A. Mietz.** 1986. Structural analysis of type II variants within the mouse intracisternal A-particle sequence family. Nucleic Acids Res. **14**:1495–1510.
50. **Madden, M. J., C. S. Morrow, M. Nakagawa, M. E. Goldsmith, C. R. Fairchild, and K. H. Cowan.** 1993. Identification of 5′ and 3′ sequences involved in the regulation of transcription of the human *mdr1* gene *in vivo*. J. Biol. Chem. **268**:8290–8297.
51. **Majors, J. E., and H. E. Varmus.** 1981. Nucleotide sequences at host-proviral junctions for mouse mammary tumour virus. Nature (London) **289**:253–258.
52. **Marchuk, D., M. Drumm, A. Saulino, and F. S. Collins.** 1991. Construction of T vectors, a rapid and general system for direct cloning of unmodified PCR products. Nucleic Acids Res. **19**: 1154.
53. **Mickley, L. A., S. E. Bates, N. D. Richert, S. Currier, S. Tanaka, F. Foss, N. Rosen, and A. T. Fojo.** 1989. Modulation of the expression of a multidrug resistance gene (*mdr-1*/P-glycoprotein) by differentiating agents. J. Biol. Chem. **264**:18031–18040.
54. **Mietz, J. A., Z. Grossman, K. K. Lueders, and E. L. Kuff.** 1987. Nucleotide sequence of a complete mouse intracisternal A-particle genome: relationship to known aspects of particle assembly and function. J. Virol. **61**:3020–3029.
55. **Moore, R., M. Dixon, R. Smith, and C. Dickson.** 1987. Complete nucleotide sequence of a milk-transmitted mouse mammary tumor virus: two frameshift suppression events are required for translation of *gag* and *pol*. J. Virol. **61**:480–490.
56. **Nusse, N., H. Theunissen, E. Wagenaar, F. Rijsewijk, A. Gennissen, A. Otte, E. Schuuring, and A. van Ooyen.** 1990. The *Wnt-1* (*int-1*) oncogene promoter and its mechanism of activation by insertion of proviral DNA of the mouse mammary tumor virus. Mol. Cell. Biol. **10**:4170–4179.
57. **Nusse, R.** 1991. Insertional mutagenesis in mouse mammary tumorigenesis. Curr. Top. Microbiol. Immunol. **171**:43–65.
58. **Nusse, R., A. van Ooyen, D. Cox, Y. K. T. Fung, and H. Varmus.** 1984. Mode of proviral activation of a putative mammary oncogene (*int-1*) on mouse chromosome 15. Nature (London) **307**:131–136.
59. **Peters, G., S. Brookes, R. Smith, M. Placzek, and C. Dickson.** 1989. The mouse homolog of the *hst/k-FGF* gene is adjacent to *int-2* and is activated by proviral insertion in some virally induced mammary tumors. Proc. Natl. Acad. Sci. USA **86**: 5678–5682.
60. **Piekarz, R. L., D. Cohen, and S. B. Horwitz.** 1993. Progesterone regulates the murine multidrug resistance *mdr*1b gene. J. Biol. Chem. **268**:7613–7616.
61. **Raymond, M., and P. Gros.** 1990. Cell-specific activity of cis-acting regulatory elements in the promoter of the mouse multidrug resistance gene *mdr1*. Mol. Cell. Biol. **10**:6036–6040.
62. **Raymond, M., E. Rose, D. E. Housman, and P. Gros.** 1990. Physical mapping, amplification, and overexpression of the mouse *mdr* gene family in multidrug-resistant cells. Mol. Cell. Biol. **10**:1642–1651.
63. **Robbins, J., B. J. Blondel, D. Gallahan, and R. Callahan.** 1992. Mouse mammary tumor gene *int-3*: a member of the *notch* gene family transforms mammary epithelial cells. J. Virol. **66**:2594–2599.
64. **Roelink, H., E. Wagenaar, S. Lopes Da Silva, and R. Nusse.** 1990. *Wnt-3*, a gene activated by proviral insertion in mouse mammary tumors, is homologous to *int-1*/*wnt-1* and is normally expressed in mouse embryos and adult brain. Proc. Natl. Acad. Sci. USA **87**:4519–4523.
65. **Rothenberg, M. L., L. A. Mickley, D. E. Cole, F. M. Balis, T. Tsuruo, D. G. Poplack, and A. T. Fojo.** 1989. Expression of the *mdr-1*/P-170 gene in patients with acute lymphoblastic leukemia. Blood **74**:1388–1395.
66. **Sambrook, J., E. F. Fritsch, and T. Maniatis.** 1989. Molecular cloning: a laboratory manual, 2nd ed. Cold Spring Harbor Laboratory Press, Cold Spring Harbor, N.Y.
67. **Schinkel, A. H., M. E. M. Roelofs, and P. Borst.** 1991. Characterization of the human *MDR3* P-glycoprotein and its recognition by P-glycoprotein-specific monoclonal antibodies. Cancer Res. **51**:2628–2635.
68. **Shen, D., A. Fojo, J. E. Chin, I. B. Roninson, N. Richert, I. Pastan, and M. M. Gottesman.** 1986. Human multidrug-resistant cell lines: increased *mdr1* expression can precede gene amplification. Science **232**:643–645.
69. **Sheng-Ong, G. L. C., and M. D. Cole.** 1982. Differing populations of intracisternal A-particle genes in myeloma tumors and mouse subspecies. J. Virol. **42**:411–421.
70. **Takatori, T., M. Ogura, and T. Tsuruo.** 1993. Purification and characterization of NF-R2 that regulates the expression of the human multidrug resistance (MDR1) gene. Jpn. J. Cancer Res. **84**:298–303.
71. **Teeter, L. D., F. F. Becker, F. V. Chisari, D. Li, and M. T. Kuo.** 1990. Overexpression of the multidrug resistance gene *mdr3* in spontaneous and chemically induced mouse hepatocellular carcinomas. Mol. Cell. Biol. **10**:5728–5735.
72. **Teeter, L. D., T. Eckersberg, Y. Tsai, and M. T. Kuo.** 1991. Analysis of the chinese hamster P-glycoprotein/multidrug resistance gene *pgp1* reveals that the AP-1 site is essential for full promoter activity. Cell Growth Differ. **2**:429–437.
73. **Ueda, K., C. Cardarelli, M. M. Gottesman, and I. Pastan.** 1987. Expression of a full-length cDNA clone from the human *MDR1* gene confers resistance to colchicine, doxorubicin and vinblastine. Proc. Natl. Acad. Sci. USA **84**:3004–3008.
74. **Ueda, K., D. P. Clark, C.-J. Chen, I. B. Roninson, M. M. Gottesman, and I. Pastan.** 1987. The human multidrug resistance (*mdr1*) gene: cDNA cloning and transcription initiation. J. Biol. Chem. **262**:505–508.
75. **Ueda, K., I. Pastan, and M. M. Gottesman.** 1987. Isolation and sequence of the promoter of the human multidrug-resistance (*mdr1*) gene. J. Biol. Chem. **262**:17432–17436.

76. **van der Bliek, A. M., P. M. Kooiman, C. Schneider, and P. Borst.** 1988. Sequence of *mdr3* cDNA encoding a human P-glycoprotein. Gene **71:**401–411.
77. **Yanagawa, S.-I., K. Kakimi, H. Tanaka, A. Murakami, Y. Nakagawa, Y. Kubo, Y. Yamada, H. Hiai, K. Kuribayashi, T. Masuda, and A. Ishimoto.** 1993. Mouse mammary tumor virus with rearranged long terminal repeats causes murine lymphomas. J. Virol. **67:**112–118.
78. **Ymer, S., W. Q. J. Tucker, C. J. Sanderson, H. D. Campbell, and I. G. Young.** 1985. Constitutive synthesis of interleukin-3 by leukaemia cell line WEHI-3B is due to retroviral insertion near the gene. Nature (London) **317:**255–258.
79. **Yu, L., D. Cohen, R. L. Piekarz, and S. B. Horwitz.** 1993. Three distinct nuclear protein binding sites in the promoter of the murine multidrug resistance *mdr*1b gene. J. Biol. Chem. **268:** 7520–7526.